Biointerface Research in Applied Chemistry
Open-Access Journal (ISSN: 2069-5837)

Article
Volume 13, Issue 2, 2023, 155
https://doi.org/10.33263/BRIAC132.155

Identification of Potential Semisynthetic Andrographolide Derivatives to Combat COVID-19 by Targeting the SARS-COV-2 Spike Protein and Human ACE2 Receptor– An *In-silico* Approach

Veerasamy Ravichandran [1,2]

[1] Faculty of Pharmacy; AIMST University, Semeling-08100, Malaysia
[2] Centre of Excellence for Biomaterials Science, AIMST University, Semeling-08100, Bedong, Malaysia
* Correspondence: ravichandran_v@aimst.edu.my (V.R.);

Scopus Author ID 16067441600
Received: 13.01.2022; Accepted: 13.02.2022; Published: 28.03.2022

Abstract: Severe acute respiratory syndrome coronavirus-2 (SARS-CoV-2) is the causal factor for the current deadly infectious disease CoVID-19. There is no specific drug available for treating COVID-19 other than some vaccines approved for prevention. However, a lot of research is in progress to prove the anti-COVID-19 potential of natural and synthetic compounds. Objective: The present study was aimed to identify the anti-COVID-19 potential of andrographolide (AGP) derivatives by *in-silico* molecular interaction study. Seventeen AGP derivatives were screened for drug-likeness, ADME, and toxicity profile using *in-silico* online tools. Then the filtered AGP were subjected to molecular docking using the PyRx tool integrated with AutoDock Vina software. Compounds AGP 15, 14, and 10 have been identified as promising binding molecules for both S and ACE2, preventing the interaction between S and ACE2. AGP-15 had shown a −8.4 Kcal/mol binding/docking score for S, AGP-10 and 14 showed a -8.3 and -8.2 Kcal/mol binding/docking score for ACE2. Overall results indicated that AGP derivatives 15 and 14 might be the best candidates to battle COVID-19. However, further studies like dynamic molecular studies and pharmacological screenings are essential to confirm the stability and action potential of AGP derivatives 14 and 15 as a lead against COVID-19.

Keywords: SARS-CoV-2; COVID-19; andrographolide; molecular docking; spike protein; angiotensin-converting enzyme 2.

1. Introduction

Coronavirus disease−2019 (COVID-19) is one of the most destructive pandemics in the 21st century. It is caused by severe acute respiratory syndrome coronavirus-2 (SARS-CoV-2) and was first identified in Wuhan, China. The WHO reports >233 million infected cases and >4.7 million deaths from SARS-CoV-2 until 1st October 2021 [1]. Like another virus, there are several proteins, like Main protease (Mpro), papain-like protease (PLpro), spike glycoprotein (S), RNA-dependent RNA polymerase (RdRp), envelop protein (E), membrane protein (M), and nucleocapsid (NSP), are responsible for virus interaction with the host, and replication of virus genomes in the host cell [2–4]. Though, human angiotensin-converting enzyme 2 (ACE2) is responsible for viral entry and fusion [4].

Andrographolide (AGP) is a significant bioactive phytoconstituent present in various *Andrographis paniculata* and family Fabaceae. Its important reported pharmacological effects

are anti-cancer, anti-inflammatory, etc. anti-microbial, anti-hepatotoxic, and antiviral to treat dengue chikungunya, swine flu, influenza. AGP is also shown potential in treating upper respiratory tract infections [5]. The published literature indicated that *A.paniculata* extract or AGP-containing medicine had been recommended for COVID-19 [6,7]. Some of the other reported studies also indicated the potential of AGP against COVID-19 [8–18]. Some researchers reported that AGP and its natural analogs had less binding affinity than remdesivir or other phytochemicals such as curcumin [8,10]. In addition, andrographolide and the major bioactive compounds of *A. paniculata* may have additional pleiotropic effects on post-viral infection due to their reported anti-inflammatory and immunomodulatory properties [19–24].

More than that, there is no specific drug to treat COVID-19; further, considering the risk factors associated with this disease; there is an urgent need to design a new drug to limit this disease transmission [25]. Meanwhile, researchers are utilizing the power of artificial intelligence in drug repurposing, finding out a hit or a lead molecule, and designing a drug to combat COVID-19 [26-48]. Hence, we have aimed to explore the binding affinity of semisynthetic and designed AGP derivatives towards SARS-CoV-2 proteins and human ACE2 using molecular docking study with the hypothesis that the semisynthetic and designed AGP derivatives would have better interaction affinity towards the main targets of COVID-19 disease than AGP, remdesivir, and hydroxychloroquine. The current study provides some preliminary scientific evidence for using AGP derivatives to combat SARS-CoV-2 by interacting with spike protein and human ACE2 receptors. Though, additional *in-vitro* and *in-vivo* experimental studies must be done to confirm the anti-COVID potential of AGP derivatives.

2. Materials and Methods

The modelling software Chem Office-16 (http://www.cambridgesoft.com/Ensemble_for_Chemistry/details/Default.aspx?fid=16), Discovery Studio Visualizer 3.0 (https://discover.3ds.com/discovery-studio-visualizer-download), Swiss Protein Data Base Viewer (https://spdbv.vital-it.ch/), PyRx (https://pyrx.sourceforge.io/), AutoDock Vina (http://vina.scripps.edu/) and online tool Swiss ADME (http://www.swissadme.ch/), ProTox-II (https://tox-new.charite.de/protox_II/) was used in the study. The 3D structures of SARS-CoV-2 proteins: spike glycoprotein (S, PDB: 6M0J) and ACE2 (ACE2, PDB: 6M18) were downloaded from Protein Data Bank (https://www.rcsb.org/).

2.1. Preparation of ligands.

The structure of AGP derivatives was drawn and converted to its 3D form in Chem Office-16 and then saved as .sdf file for further use. Physicochemical, pharmacokinetics, and toxicity of AGP derivatives were calculated with the help of online tools such as SwissADME and ProTox-II.

2.2. Active site predictions.

The active binding site of the S protein and ACE2 receptor was identified with the help of gained information from the literature [49,50].

2.3. Preparation of proteins.

The crystallographic structures of SARS-CoV-2 proteins S and human ACE2 receptors were checked for any missed atoms or chains using Swiss Protein Data Base Viewer and corrected. Then, water and other heteroatoms were removed, polar hydrogens were added, and saved as PDB format for docking study [51].

2.4. Docking studies.

AGP derivatives and protein structures were uploaded in the Virtual Screening software interface PyRx 0.8 utilizes Autodock Vina and Autodock 4.2. AGP structures were then energy-minimized (200 iterations) with the MMFF94 force field. Local search method Broyden-Fletcher-Goldfarb-Shanno (BFGS) used to energy minimization of protein. Then, with the help of the auto dock tool, both protein and ligand molecules were converted to the '.pdbqt' format. The active binding site grid box was created around the active site amino acids, which details were extracted from published literature [51]. All other software parameters were kept as default. The ligand was considered flexible and the receptor as rigid. PyRx uses the Lamarckian genetic algorithm as a scoring function. Visualization of the docked poses was executed using Discovery Studio Visualizer 3.0. The best confirmer was selected based on the docking score and better non-covalent bond interaction. The best docking pose and ligand-protein interaction pictures were collected and saved [52].

3. Results and Discussion

The main objective of the present study was to identify the potential semisynthetic andrographolide derivatives to inhibit SARS-CoV-2 infection. In the current study, we have selected an important target protein of the SARS-CoV-2 genome, spike glycoprotein (S, PDB: 6M0J), and human ACE2 receptor (ACE2, PDB: 6M18). Viral spike proteins bind and fuse with the host ACE-2 receptor, and then viruses enter the host cell. So, the S and ACE2 are two crucial targets to inhibit viral entry into the host. Hence, we have selected these two enzymes for our current study to explore the interaction efficiency of semisynthetic AGP derivatives on the SARS-CoV-2 virus. The present research work studied the molecular interactions of AGP derivatives with S and ACE2. In this study, we have used 17 semisynthetic AGP derivatives (Figure 1), including andrographolide, remdesivir, and hydroxychloroquine, as reference drugs. Out of 17 AGP derivatives, nine were taken from the earlier reported study [53] and 8 were our own designed compounds. PDB structures of spike protein and ACE2 receptor were given in Figure 2. All the AGP derivatives interacted with S and ACE2 by docking in the binding pocket cavity.

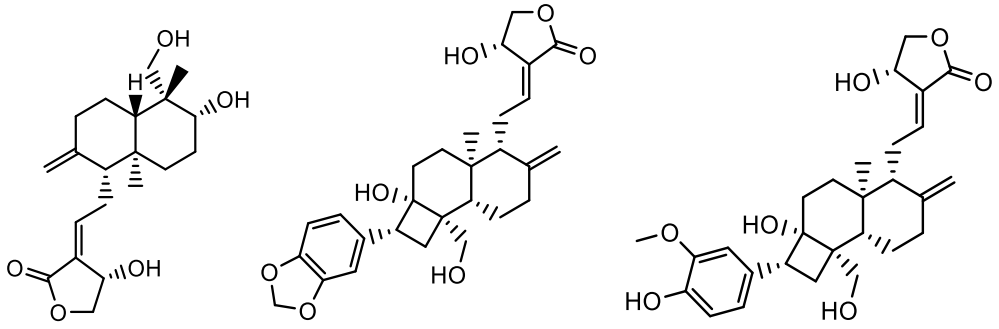

1 2 3

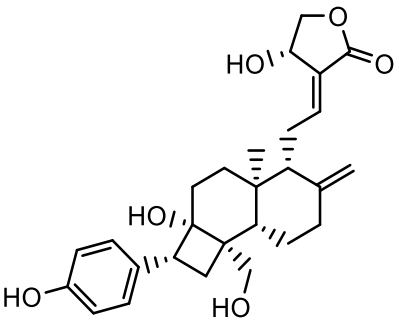

4

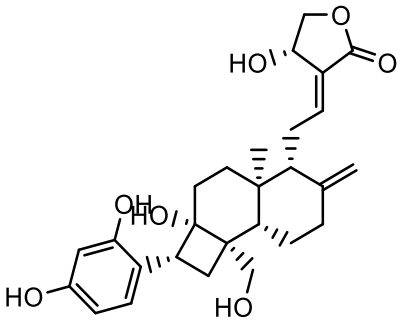

5

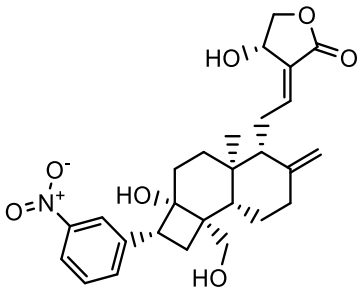

6

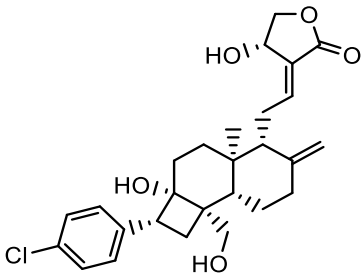

7

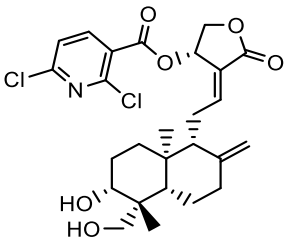

8

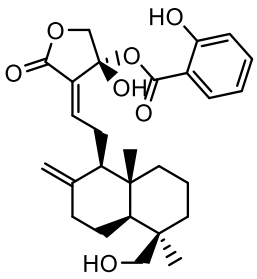

9

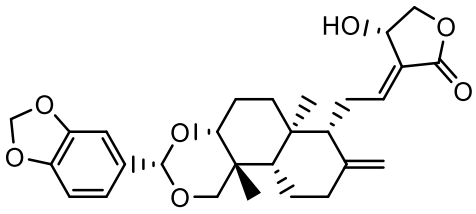

10

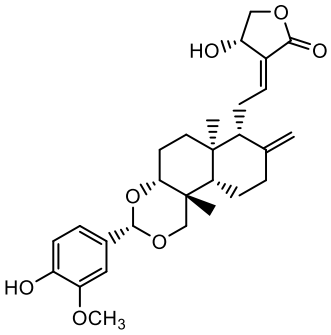

11

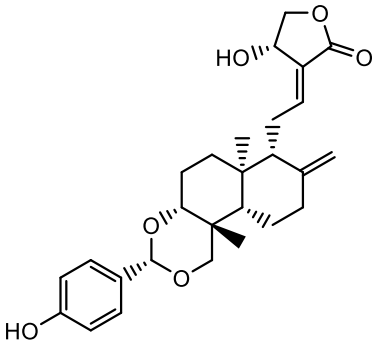

12

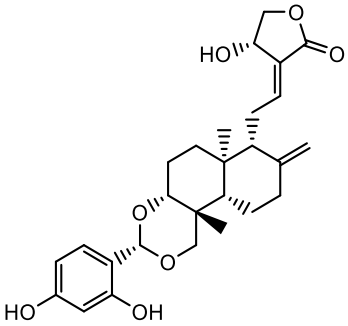

13

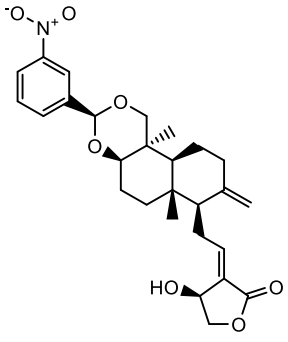

14

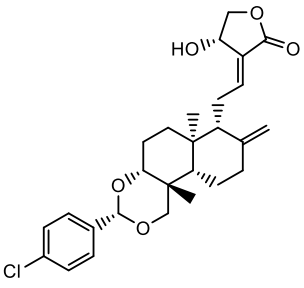

15

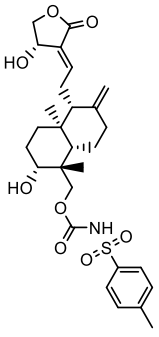

16

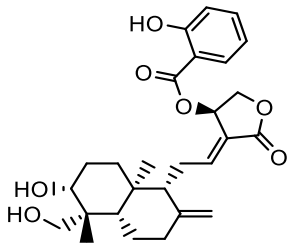

17

Figure 1. Structures of AGP derivatives.

The drug-likeness and ADMET properties of 17 AGP derivatives were predicted using SwissADME and ProTox-II online tools, respectively. Except AGP8, 14, 15, and 16, all other derivatives followed Lipinski's rule of five. In that, AGP8 and 16 have a molecular weight > 500, and AGP14 and 15 have a LogP value > 5, but the differences are negligible. All the AGP derivatives exhibited GI absorption except AGP6 and 16. All the APG derivatives are free from hepatotoxicity, carcinogenicity, mutagenicity, and cytotoxicity, and acute oral toxicity for all compounds estimated as class IV or better than that. Hence all the 17 derivatives, including AGP were considered for docking studies.

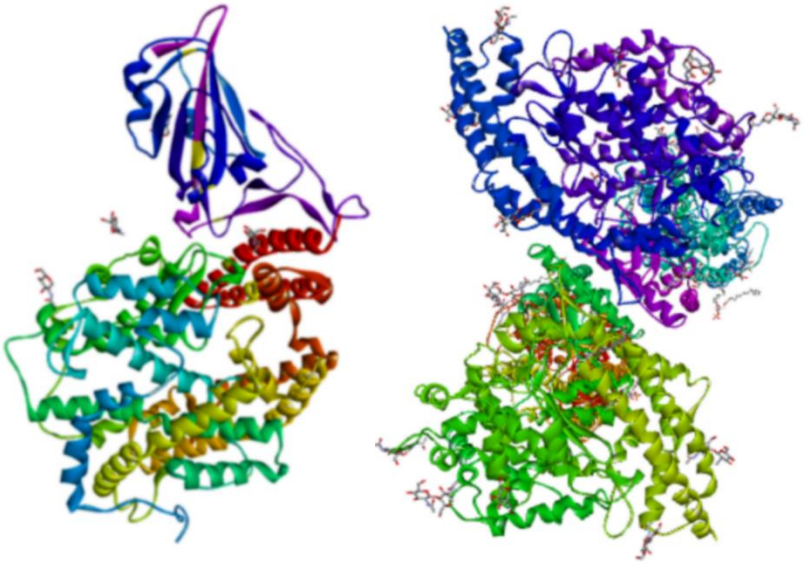

A B

Figure 2. Structures of SARS-CoV-2 proteins. A – Spike protein (PDB: 6M0J), B – ACE2 (PDB: 6M18).

3.1. Docking study.

The coordinate/center of the x, y, and z axes of the grid box of both protein active binding sites is given in Table 1. The present docking study protocol was validated by repeated docking the reference compounds HCQ and REM with the same protein separately. All binding confirmations of the repeated-docked ligands were interacted with the same residues of protein binding pocket and had the root means square deviation (RMSD) below 2 Å.

Table 1. Coordinate the x, y, and z centers of grid boxes of protein targets with dimensions.

Protein molecule	x- centers (Dimension)	y-centers (Dimension)	z-center (Dimension)
Spike Protein	-31.72 (25 Å)	24.86 (25 Å)	30.08 (25 Å)
ACE2	134.14 (25 Å)	154.60 (25 Å)	214.63 (25 Å)

Then the docking studies for AGP derivatives were carried out using PyRx 0.8 tool. All AGP derivatives interacted with the binding pocket cavity amino acid residues of the S and ACE2 by docking. The best binding affinity for all AGP derivatives with S-RBD was found in the range -5.6 to -8.4 kcal/mol. However, binding affinity with ACE2 was found in the range of -6.2 to -8.3 kcal/mol. Compound AGP15 exhibited a binding affinity value of -8.4 kcal/mol. In comparison, AGP had a binding affinity value of -6.7 kcal/mol against S. Meanwhile, compound AGP10 exhibited a -8.3 kcal/mol. In comparison, AGP had a binding affinity value of -6.5 kcal/mol against ACE2. The binding affinity/energy of the AGP derivatives towards S and ACE2 receptors are shown in Table 2, and the details of the amino acid residue of proteins interacted with AGP derivatives and the reference drugs are given in Table 3. The docking output files were analyzed for 3D interaction, docking pose on hydrogen bond donor surface, and 2D interaction using discovery studio visualizer 3. The docking pose and interaction images of REM, HCQ, and AGP derivatives have the highest binding energy with S and ACE2 are given in Figures 3 and 4, respectively.

Table 2. The binding affinity of andrographolide derivatives with protein targets.

S. No	Compounds	Binding affinity (kcal/mol)	
		Spike RBD	ACE2
1	1 (AGP)	-6.7	-6.5
2	2	-7.4	-7.5
3	3	-7.0	-7.0
4	4	-7.0	-7.1
5	5	-7.2	-6.9
6	6	-7.4	-7.7
7	7	-7.3	-7.4
8	8	-7.3	-7.0
9	9	-7.4	-6.2
10	10	-7.1	-8.3
11	11	-7.4	-7.7
12	12	-7.2	-7.8
13	13	-7.7	-7.2
14	14	-7.7	-8.2
15	15	-8.4	-8.0
16	16	-6.3	-7.3
17	17	-5.6	-7.1
18	REM	-6.7	-6.6
19	HCQ	-5.4	-5.3

RBD-Receptor binding domain, AGP – Andrographolide, REM- Remdesivir, HCQ - Hydroxychloroquine

Table 3. Amino acids of protein targets involved in interactions with AGP derivatives.

Bonding interaction	Spike receptor	ACE2	Spike receptor	ACE2
	Amino acids involved in the interaction			
HCQ			**REM**	
Hydrogen bond	Phe515	Asn159, Asn134	Arg355, Arg355, Arg355, Arg466, Arg466, Ser514, Phe464	Asn690, Sn690, Asn690, Asp136
Hydrophobic	Phe464, Phe429	Glu160, Val691, Trp163	Phe429, Pro426	Trp163, Lys689, Pro688, Lys689
Others	Asp428 (C), Glu516 (E)	Asp136 (C), Asp157 (C), Glu160 (E)	Phe464 (C)	Asn690 (C)
1			**2**	
Hydrogen bond	Arg355, Asp428	Asn690, Asn690	Arg355, Tyr396, Glu516	Asn134, Asn690
Hydrophobic	Phe464	--	Pro426, Phe464	Pro135
Others	--	Glu160 (C)	--	--
3			**4**	
Hydrogen bond	Arg355, Arg357,	Asn134, Ser692, Asn690, Asn690	Asn354, Arg355	Asn134, Glu160,

Bonding interaction	Spike receptor	ACE2	Spike receptor	ACE2
	Amino acids involved in the interaction			
HCQ			**REM**	
	Arg355			Asn690
Hydrophobic	Tyr396 -	Pro135	--	Pro135
Others	Trp353 (C), Arg355 (Pi-Cation; Pi-Donor Hydrogen Bond)	--	Arg355 (E)	--
5			**6**	
Hydrogen bond	Asn334, Lys356, Asn360, Asn360, Ser359	Leu156, Asp157, Asn690	Arg355, Arg466	Asn690, Glu140, Asn159
Hydrophobic	Pro337, Cys361	Trp163, Trp163, Pro135	--	Pro135
Others	Ser359 (C)	Ser155 (C), Glu160 (C)	--	Asn690 (C)
7			**8**	
Hydrogen bond	Arg466	Asn134, Ser692, Glu160, Asn690	Arg355, Arg355	Lys689, Asn690
Hydrophobic	Tyr396, Phe464	Lys689, Pro135	Leu518	--
Others	Arg355 (C)			Glu160 (C)
9			**10**	
Hydrogen bond	Thr430	Glu160	Arg355, Arg355, Tyr396, Glu516	Asn690
Hydrophobic	Tyr396, Leu517	Asn159, Glu160	Phe464	Pro688, Pro135
Others	--	Glu160, Glu160	--	--
11			**12**	
Hydrogen bond	Arg466	--	Thr430, Leu517	--
Hydrophobic	Arg357, Arg357	Pro688, Trp163, Pro135	--	Pro688, Lys689, Pro135
Others	--	Ala687 (C), Asn690 (C), Asp136 (E)	--	--
13			**14**	
Hydrogen bond	Lys356, Arg357, Arg357	Gln661, Glu699	Arg357, Ser359, Asn360	--
Hydrophobic	Arg355	Phe655, Ala687, Pro688, Lys689	Arg357	Pro688, Pro135
Others	--	--	Leu335 (C)	Trp163 (C)
15			**16**	
Hydrogen bond	Arg355, Asp428	Asn690	Arg355, Arg355, Arg355, Arg355, Arg357	Lys689
Hydrophobic	Phe464	Pro688, Pro135	Pro426	Trp163, Trp163, Lys689
Others	Ser514 (C), Thr430 (C)	--	--	--
17				
Hydrogen bond	Thr430, Glu516	Asn159, Gln616, Ile694	--	--
Hydrophobic	Phe464	Tyr158, Tyr255, Pro696	--	--
Others	--	--	--	--

E – Electrostatic, C – carbon-hydrogen bond

3.2. Binding to spike protein receptor-binding domain.

The protein-protein interaction between the subunits of the spike protein and the ACE-2 receptor active site is responsible for the viral entry into the host cell since the receptor-binding domain spike, and ACE2 can be targeted to identify an effective treatment strategy for COVID-19. In the current study, the reference drugs REM and HCQ had shown binding affinity of -6.7 and -5.4 kcal/mol towards S.

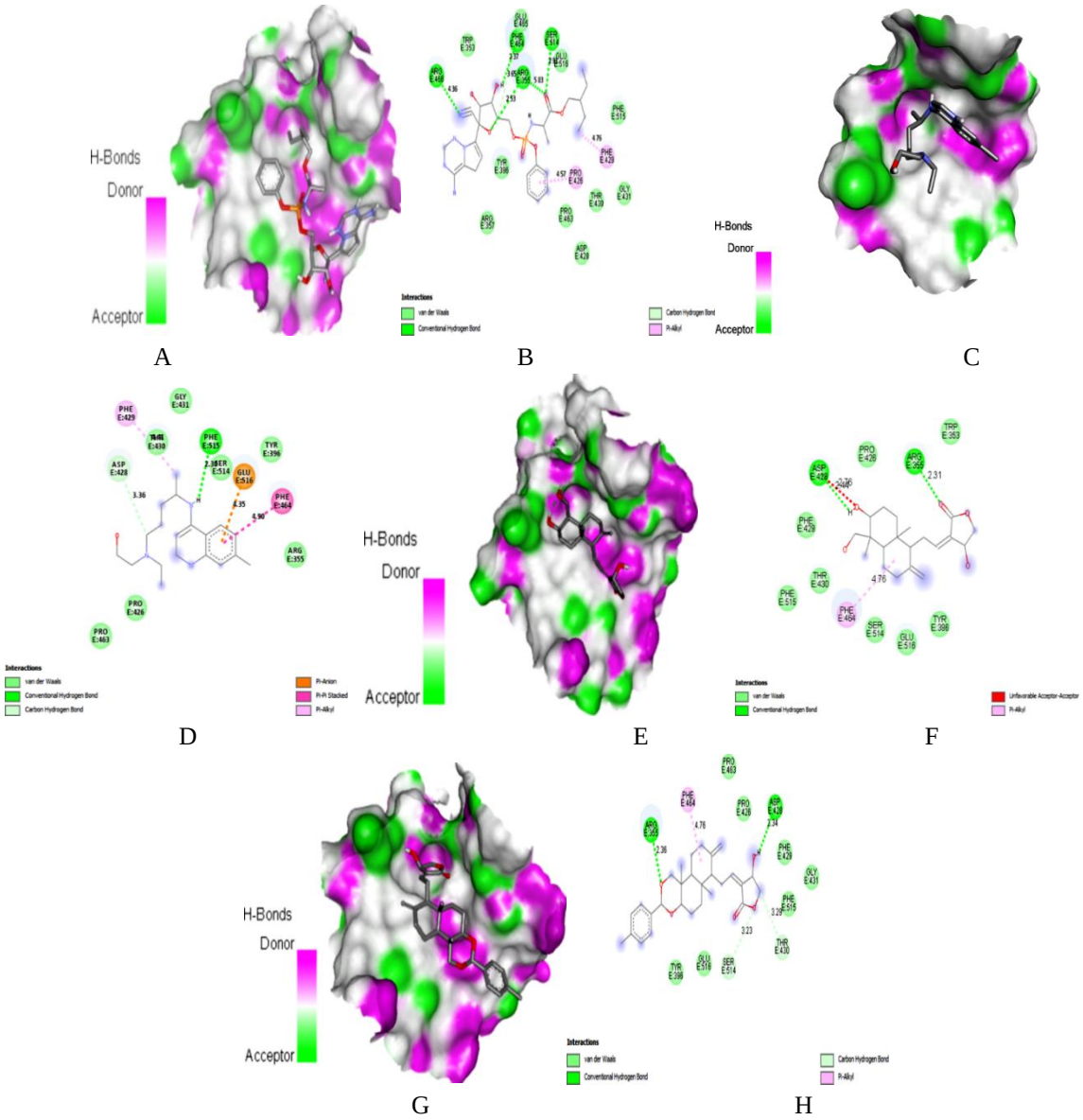

Figure 3. Docking with spike protein RBD: A) Docking pose of REM on hydrogen bonding surface, B) 2D interaction of REM, C) Docking pose of HCQ on hydrogen bonding surface, D) 2D interaction of HCQ, E) Docking pose of AGP on hydrogen bonding surface, F) 2D interaction of AGP, G) Docking pose of AGP-15 on hydrogen bonding surface, H) 2D interaction of AGP-15.

The binding affinity results given in Table 2 showed that the unsubstituted natural AGP (AGP1) was not the most suitable one among the investigated derivatives for potent interaction with S. Fourteen of 16 AGP derivatives, except AGP16 and 17, were shown a better binding affinity towards S than REM and AGP. Meanwhile, all the 16 AGP derivatives had shown a better binding affinity towards S than HCQ. AGP15 was placed at rank 1 with the highest binding affinity -8.4 kcal/mol for S, followed by AGP13 and 14 with -7.7 kcal/mol.

Seven H-bonds at Arg355 (3 bonds: 2.36, 2.53, 2.70 Å), Arg466 (2 bonds: 2.54, 2.76 Å), Ser514 (2.91 Å), and Phe464 (2.37 Å), two hydrophobic bond interactions at Phe429 and Pro426, and a C-H bond at Phe464 were observed in the binding complex of REM with S (Figure 3A and 3B). Whereas HCQ had one H-bond at Phe515 (2.30 Å), two hydrophobic interactions at Phe464 and Phe429, one C-H bond interaction at Asp428, and an electrostatic interaction at Glu516 (E) with S (Figure 3C and 3D).

AGP formed two H-bonds with Arg355 (2.31 Å) and Asp428 (2.44 Å), and hydrophobic interaction with Phe464 (Figure 3E and 3F). The interaction between AGP15 and S is strengthened by two hydrogen bonds with residues Arg355 (2.36 Å) and Asp428 (2.34 Å), one hydrophobic interaction with Phe464, and two C-H interactions with residues Ser514 and Thr430 (Figure 3G and 3H). However, two AGP derivatives 13 and 14 had shown the same binding affinity with S. AGP13 formed three H-bonds and a hydrophobic bond, whereas AGP14 had three H-bonds, one hydrophobic. A C-H bond interaction within the binding cleft of S. Identified AGP derivatives AGP15, 13 and 14 showed more stable H-bonds and hydrophobic compared to reported antivirals. The common amino acid residues of S involved in the H-bond and hydrophobic interaction with maximum AGP derivatives were Arg355, Arg357, Asp428, and Arg466. The other amino acid residues of S involved in the van der Waals interaction with AGP derivatives were Pro426, Phe429, Thr430, Ser514, Phe515, and Glu516. Our current study results differ from Lakshmi *et al*. (2020) [13] and Maurya *et al*. (2020) [14] since they reported that the natural AGP analogs interacted with Tyr28, Phe59, and Thr761 of spike glycoprotein. The attaching ability of SARS-CoV-2 to the host ACE2 can be inhibited when AGP derivatives bind to the S active site, thus reducing the further transmission of the virus. The high binding affinity of AGP derivatives towards S indicates that they can be a promising lead compound as S inhibitors to treat COVID-19 infection.

3.3. Binding to ACE2.

In the current study, REM and HCQ were shown a binding affinity of -6.6 and -5.3 kcal/mol against ACE2. The binding affinity results given in Table 2 showed that the unsubstituted natural AGP (AGP1) was not the most suitable one among the investigated derivatives for potent interaction with ACE2. Except for AGP9, all other derivatives were shown an improved binding affinity towards ACE2 than REM and AGP; however, all the 16 AGP derivatives had better binding affinity against ACE2 than HCQ. AGP10 was placed at rank 1 with the highest binding affinity -8.3 kcal/mol for ACE2, followed by AGP14 and 15 with -8.2 and -8.0 kcal/mol, respectively. REM showed four H-bonds at Asn690 (3 bonds: 2.43, 2.63, 3.06 Å) and Asp136, four hydrophobic bond interactions at Trp163, Lys689 (2 bonds), and Pro688, and a C-H bond at Asn690 with ACE2 (Figure 4A and 4B). Whereas HCQ had two H-bonds at Asn159 (2.47 Å) and Asn134 (3.05 Å), three hydrophobic interactions at Glu160, Val691, and Trp163, two C-H bond interactions at Asp136 and Asp157, and an electrostatic interaction at Glu160 with ACE2 (Figure 4C and 4D).

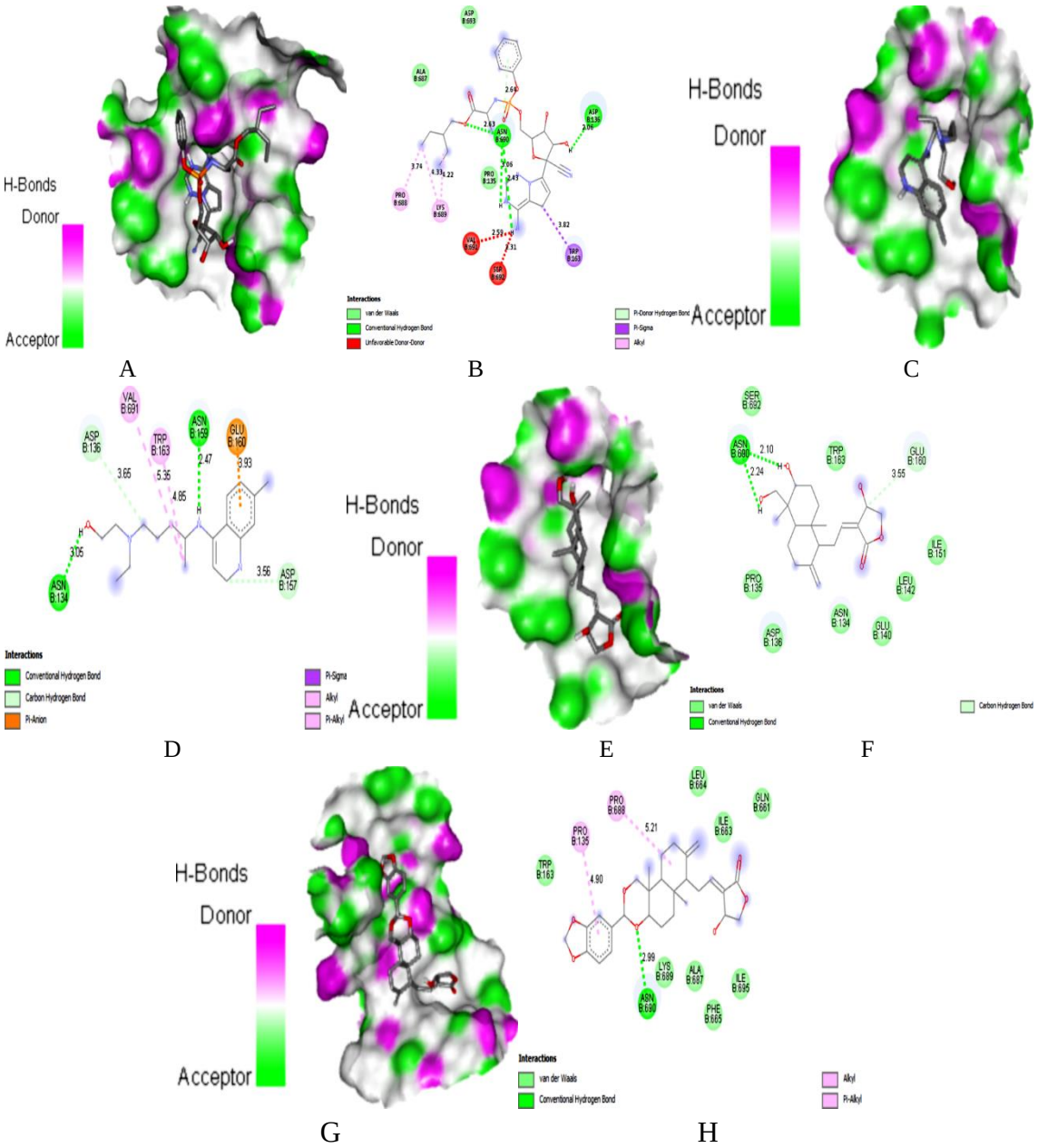

Figure 4. Docking with ACE2: A) Docking pose of REM on hydrogen bonding surface, B) 2D interaction of REM, C) Docking pose of HCQ on hydrogen bonding surface, D) 2D interaction of HCQ, E) Docking pose of AGP on hydrogen bonding surface, F) 2D interaction of AGP, G) Docking pose of AGP-10 on hydrogen bonding surface, H) 2D interaction of AGP-10.

AGP formed two H-bonds with Asn690 (2.10, 2.24 Å) and a C-H interaction with Glu160 (Figure 4E and 4F). The interaction between AGP10 and ACE2 is strengthened by a hydrogen bond with Asn690 (2.98 Å) and two hydrophobic interactions with Pro688 and Pro135 (Figure 4G and 4H). However, AGP14 formed two hydrophobic bonds at Pro688 and Pro135 and a C-H bond interaction at Trp163 with ACE2. Identified AGP derivatives 10, 14, and 15 showed more stable H-bonds and hydrophobic than reported antivirals. The attaching ability of SARS-CoV-2 to the host ACE2 can be inhibited when AGP derivatives bind to the ACE2 binding site, thus reducing the further transmission of the virus. The high binding affinity of AGP derivatives towards ACE2 indicates that they can be a promising lead compound to treat COVID-19 infection.

Almost all compounds showed interactions with key amino acid residues of the S protein (Arg355, Lys356, Arg357, Asn360, Phe429, Pro426, Asp428, Phe464, Arg466,

Ser514, Leu517) and ACE2 receptor (Asn134, Pro135, Glu160, Trp163, Pro688, Lys689, Asn690). However, reference drugs and major AGP derivatives involved in interaction with the main amino acid residues of S were Arg355, Arg357, and Phe464, and the main amino acid residues of ACE2 were Pro135, Glu160, Trp163, Lys689, Asn690.

4. Conclusions

The information generated from the present docking results can provide insights into exploring potential drugs against SARS-CoV-2 from andrographolide. Pharmacokinetic, drug-likeness properties, and docking studies revealed that AGP15 and AGP14 might be the best candidates for designing and developing new antiviral drugs. Thus, we conclude that these AGP derivatives can be utilized as potential anti-COVID-19 candidates. Further innovation and development of these compounds against coronavirus can bring good antiviral candidates to treat SARS-CoV-2 infection.

Funding

This research received no external funding.

Acknowledgments

The authors would like to thank AIMST University for providing the necessary facilities to carry out this research work.

Conflicts of Interest

The authors declare no conflict of interest.

References

1. WHO Coronavirus (COVID-19) Dashboard. https://covid19.who.int (Accessed on 15th October **2021).**
2. Stadler, K.; Masignani, V.; Eickmann, M.; Becker, S.; Abrignani, S.; Klenk, H.D.; Rappuoli, R. SARS—Beginning to Understand a New Virus. *Nature Reviews Microbiology* **2003**, *1*, 209–218, https://doi.org/10.1038/nrmicro775.
3. Li, F.; Li, W.; Farzan, M.; Harrison, S.C. Structure of SARS Coronavirus Spike Receptor−binding Domain Complexed with Receptor. *Science* **2005**, *309*, 1864–1868, https://doi.org/10.1126/science.1116480.
4. Elfiky, A.A. Anti-HCV, Nucleotide Inhibitors, Repurposing against COVID-19. *Life Sci* **2020**, *248*, https://doi.org/10.1016/j.lfs.2020.117477.
5. Jayakumar, T.; Hsieh, C.-Y.; Lee, J.-J.; Sheu, J.-R. Experimental and Clinical Pharmacology of Andrographis Paniculata and Its Major Bioactive Phytoconstituent Andrographolide. *Evid Based Complement Alternat Med* **2013**, *2013*, https://doi.org/10.1155/2013/846740.
6. Wipatayotin, A. Local Herb Study on Covid-19 Patients to Continue. *Bangkok Post*. https://www.bangkokpost.com/thailand/general/2058723/local-herb-study-on-covid-19-patients-to-continue (Accessed on 15th October **2021**).
7. Wang, C.; Sun, S.; Ding, X. The Therapeutic Effects of Traditional Chinese Medicine on COVID-19: A Narrative Review. *Int J Clin Pharm* **2021**, *43*, 35–45, https://doi.org/10.1007/s11096-020-01153-7.
8. Shi, T.-H.; Huang, Y.-L.; Chen, C.-C.; Pi, W.-C.; Hsu, Y.-L.; Lo, L.-C.; Chen, W.-Y.; Fu, S.-L.; Lin, C.-H. Andrographolide and Its Fluorescent Derivative Inhibit the Main Proteases of 2019-NCoV and SARS-CoV through Covalent Linkage. *Biochem Biophys Res Commun* **2020**, *533*, 467–473, https://doi.org/10.1016/j.bbrc.2020.08.086.
9. Kanjanasirirat, P.; Suksatu, A.; Manopwisedjaroen, S.; Munyoo, B.; Tuchinda, P.; Jearawuttanakul, K.; Seemakhan, S.; Charoensutthivarakul, S.; Wongtrakoongate, P.; Rangkasenee, N.; Pitiporn, S.; Waranuch, N.; Chabang, N.; Khemawoot, P.; Sa-ngiamsuntorn, K.; Pewkliang, Y.; Thongsri, P.; Chutipongtanate, S.; Hongeng, S.; Borwornpinyo, S.; Thitithanyanont, A. High-Content Screening of Thai Medicinal Plants Reveals Boesenbergia Rotunda Extract and Its Component Panduratin A as Anti-SARS-CoV-2 Agents. *Sci Rep* **2020**, *10*, https://doi.org/10.1038/s41598-020-77003-3.

10. Alazmi, M.; Motwalli, O. Molecular Basis for Drug Repurposing to Study the Interface of the S Protein in SARS-CoV- 2 and Human ACE2 through Docking, Characterization, and Molecular Dynamics for Natural Drug Candidates. *J Mol Model* **2020**, *26*, https://doi.org/10.1007/s00894-020-04599-8.
11. Enmozhi, S.K.; Raja, K.; Sebastine, I.; Joseph, J. Andrographolide as a Potential Inhibitor of SARS-CoV- 2 Main Protease: An in Silico Approach. *J Biomol Struct Dyn* **2021**, *39*, 3092-3098, https://doi.org/10.1080/07391102.2020.1760136.
12. Kodchakorn, K.; Poovorawan, Y.; Suwannakarn, K.; Kongtawelert, P. Molecular Modelling Investigation for Drugs and Nutraceuticals against Protease of SARS-CoV- 2. *J Mol Graph Model* **2020**, *101*, https://doi.org/10.1016/j.jmgm.2020.107717.
13. Lakshmi, S.A.; Shafreen, R.M.B.; Priya, A.; Shunmugiah, K.P. Ethnomedicines of Indian Origin for Combating COVID-19 Infection by Hampering the Viral Replication: Using Structure-Based Drug Discovery Approach. *J Biomol Struct Dyn* **2020**, *39*, 4594-4609, https://doi.org/10.1080/07391102.2020.1778537.
14. Maurya, V.K.; Kumar, S.; Prasad, A.K.; Bhatt, M.L.B.; Saxena, S.K. Structure-Based Drug Designing for Potential Antiviral Activity of Selected Natural Products from Ayurveda against SARS-CoV- 2 Spike Glycoprotein and Its Cellular Receptor. *Virusdisease* **2020**, *31*,179-193, https://doi.org/10.1007/s13337-020-00598-8.
15. Murugan, N.A.; Pandian, C.J.; Jeyakanthan, J. Computational Investigation on Andrographis Paniculata Phytochemicals to Evaluate Their Potency against SARS-CoV- 2 in Comparison to Known Antiviral Compounds in Drug Trials. *J Biomol Struct Dyn* **2020,** *39*, 4415-4426, https://doi.org/10.1080/07391102.2020.1777901.
16. Rathinavel, T.; Thangaswamy, S.; Ammashi, S.; Kumarasamy, S. Virtual Screening of COVID-19 Drug from Three Indian Traditional Medicinal Plants through in Silico Approach. *Res J Biotechnol* **2020**, *15*.
17. Sharma, A.; Vora, J.; Patel, D.; Sinha, S.; Jha, P.C.; Shrivastava, N. Identification of Natural Inhibitors against Prime Targets of SARS-CoV- 2 Using Molecular Docking, Molecular Dynamics Simulation and MM-PBSA Approaches. *J Biomol Struct Dyn* **2020,** 1–16, https://doi.org/10.1080/07391102.2020.1846624.
18. Sukardiman; Ervina, M.; Fadhil Pratama, M.R.; Poerwono, H.; Siswodihardjo, S. The Coronavirus Disease 2019 Main Protease Inhibitor from Andrographis Paniculata (Burm. f) Ness. *J Adv Pharm Technol Res* **2020**, *11*, 157–162, https://doi.org/10.4103/japtr.JAPTR_84_20.
19. Wang, T.; Liu, B.; Zhang, W.; Wilson, B.; Hong, J.-S. Andrographolide Reduces Inflammation-Mediated Dopaminergic Neurodegeneration in Mesencephalic Neuron-Glia Cultures by Inhibiting Microglial Activation. *J Pharmacol Exp Ther* **2004**, *308*, 975–983, https://doi.org/10.1124/jpet.103.059683.
20. Li, J.; Luo, L.; Wang, X.; Liao, B.; Li, G. Inhibition of NF-KappaB Expression and Allergen-Induced Airway Inflammation in a Mouse Allergic Asthma Model by Andrographolide. *Cell Mol Immunol* **2009**, *6*, 381–385, https://doi.org/10.1038/cmi.2009.49.
21. Naik, S.R.; Hule, A. Evaluation of Immunomodulatory Activity of an Extract of Andrographolides from Andographis Paniculata. *Planta Med* **2009**, *75*, 785–791, https://doi.org/10.1055/s-0029-1185398.
22. Suresh, V.; Deepika, G.; Bantal, V.; Beedu, S.R.; Rupula, K. Evaluation of Anti-Inflammatory and Anti-Nociceptive Potentials of Andrographolide and Forskolin: In Vivo Studies. *J biol act prod nat* **2018**, *8*, 326–334, https://doi.org/10.1080/22311866.2018.1526650.
23. Li, Y.; He, S.; Tang, J.; Ding, N.; Chu, X.; Cheng, L.; Wu, J. Andrographolide Inhibits Inflammatory Cytokines Secretion in LPS-Stimulated RAW264. 7 Cells through Suppression of NF-KB/MAPK Signaling Pathway. *Evid Based Complement Alternat Med* **2017**, *2017*, https://doi.org/10.1155/2017/8248142.
24. Wang, W.; Wang, J.; Dong, S.-F.; Liu, C.-H.; Italiani, P.; Sun, S.-H.; Xu, J.; Boraschi, D.; Ma, S.-P.; Qu, D. Immunomodulatory Activity of Andrographolide on Macrophage Activation and Specific Antibody Response. *Acta Pharmacol Sin* **2010**, *31*, 191–201, https://doi.org/10.1038/aps.2009.205.
25. Enayatkhani, M.; Hasaniazad, M.; Faezi, S.; Gouklani, H.; Davoodian, P.; Ahmadi, N.; Einakian, M.A.; Karmostaji, A.; Ahmadi, K. Reverse Vaccinology Approach to Design a Novel Multi-Epitope Vaccine Candidate against COVID-19: An in Silico Study. *J Biomol Struct Dyn* **2021**, *39*, 2857–2872, https://doi.org/10.1080/07391102.2020.1756411.
26. Cardoso, E.F.; Giacomello, T.F.; Rocha de Oliveira, L.L.; da Silva, T.A.; de Jesus Chaves Neto, A.M.; Da Silva Mota, G.V.; Souza Siqueira, M.R.; Paranhos Costa, F.L. A Combined Molecular Docking and Density Functional Theory Nuclear Magnetic Resonance Study of Trans-Dehydrocrotonin Interacting with COVID-19 Main Protease and Severe Acute Respiratory Syndrome Coronavirus 2 3C-Like Protease. *J Nanosci Nanotechnol* **2021**, *21*, 5399–5407, https://doi.org/10.1166/jnn.2021.19475.
27. Muhammad, S.; Maqbool, M.F.; Al-Sehemi, A.G.; Iqbal, A.; Khan, M.; Ullah, S.; Khan, M.T. A Threefold Approach Including Quantum Chemical, Molecular Docking and Molecular Dynamic Studies to Explore the Natural Compounds from Centaurea Jacea as the Potential Inhibitors for COVID-19. *Braz J Biol* **2021**, *83*, https://doi.org/10.1590/1519-6984.247604.
28. Suručić, R.; Tubić, B.; Stojiljković, M.P.; Djuric, D.M.; Travar, M.; Grabež, M.; Šavikin, K.; Škrbić, R. Computational Study of Pomegranate Peel Extract Polyphenols as Potential Inhibitors of SARS-CoV-2 Virus Internalization. *Mol Cell Biochem* **2021**, *476*, 1179–1193, https://doi.org/10.1007/s11010-020-03981-7.
29. Kumar, S.; Kashyap, P.; Chowdhury, S.; Kumar, S.; Panwar, A.; Kumar, A. Identification of Phytochemicals as Potential Therapeutic Agents That Binds to Nsp15 Protein Target of Coronavirus (SARS-CoV-2) That Are

Capable of Inhibiting Virus Replication. *Phytomedicine* **2021**, *85*, https://doi.org/10.1016/j.phymed.2020.153317.
30. Rajagopal, K.; Varakumar, P.; Aparna, B.; Byran, G.; Jupudi, S. Identification of Some Novel Oxazine Substituted 9-Anilinoacridines as SARS-CoV-2 Inhibitors for COVID-19 by Molecular Docking, Free Energy Calculation and Molecular Dynamics Studies. *J Biomol Struct Dyn* **2021**, *39*, 5551–5562, https://doi.org/10.1080/07391102.2020.1798285.
31. Shah, V.R.; Bhaliya, J.D.; Patel, G.M. In Silico Approach: Docking Study of Oxindole Derivatives against the Main Protease of COVID-19 and Its Comparison with Existing Therapeutic Agents. *J Basic Clin Physiol Pharmacol* **2021**, *32*, 197–214, https://doi.org/10.1515/jbcpp-2020-0262.
32. Ibrahim, M.A.A.; Abdelrahman, A.H.M.; Allemailem, K.S.; Almatroudi, A.; Moustafa, M.F.; Hegazy, M.-E.F. In Silico Evaluation of Prospective Anti-COVID-19 Drug Candidates as Potential SARS-CoV-2 Main Protease Inhibitors. *Protein J* **2021**, *40*, 296–309, https://doi.org/10.1007/s10930-020-09945-6.
33. Xu, J.; Gao, L.; Liang, H.; Chen, S.-D. In Silico Screening of Potential Anti-COVID-19 Bioactive Natural Constituents from Food Sources by Molecular Docking. *Nutrition* **2021**, *82*, https://doi.org/10.1016/j.nut.2020.111049.
34. Çakır, B.; Okuyan, B.; Şener, G.; Tunali-Akbay, T. Investigation of Beta-Lactoglobulin Derived Bioactive Peptides against SARS-CoV-2 (COVID-19): In Silico Analysis. *Eur J Pharmacol* **2021**, *891*, https://doi.org/10.1016/j.ejphar.2020.173781.
35. Dey, P. Low Bioavailability Hinders Drug Discovery against COVID-19, Guided by in Silico Docking. *Br J Pharmacol* **2021**, *178*, 741–742, https://doi.org/10.1111/bph.15325.
36. Rai, H.; Barik, A.; Singh, Y.P.; Suresh, A.; Singh, L.; Singh, G.; Nayak, U.Y.; Dubey, V.K.; Modi, G. Molecular Docking, Binding Mode Analysis, Molecular Dynamics, and Prediction of ADMET/Toxicity Properties of Selective Potential Antiviral Agents against SARS-CoV-2 Main Protease: An Effort toward Drug Repurposing to Combat COVID-19. *Mol Divers* **2021**, *25*, 1905–1927, https://doi.org/10.1007/s11030-021-10188-5.
37. Vique-Sánchez, J.L. Potential Inhibitors Interacting in Neuropilin-1 to Develop an Adjuvant Drug against COVID-19, by Molecular Docking. *Bioorg Med Chem* **2021**, *33*, https://doi.org/10.1016/j.bmc.2021.116040.
38. Kumar, D.; Kumari, K.; Vishvakarma, V.K.; Jayaraj, A.; Kumar, D.; Ramappa, V.K.; Patel, R.; Kumar, V.; Dass, S.K.; Chandra, R.; Singh, P. Promising Inhibitors of Main Protease of Novel Corona Virus to Prevent the Spread of COVID-19 Using Docking and Molecular Dynamics Simulation. *J Biomol Struct Dyn* **2021**, *39*, 4671–4685, https://doi.org/10.1080/07391102.2020.1779131.
39. Gowrishankar, S.; Muthumanickam, S.; Kamaladevi, A.; Karthika, C.; Jothi, R.; Boomi, P.; Maniazhagu, D.; Pandian, S.K. Promising Phytochemicals of Traditional Indian Herbal Steam Inhalation Therapy to Combat COVID-19-An in Silico Study. *Food Chem Toxicol* **2021**, *148*, https://doi.org/10.1016/j.fct.2020.111966.
40. Gu, Y.-Y.; Zhang, M.; Cen, H.; Wu, Y.-F.; Lu, Z.; Lu, F.; Liu, X.-S.; Lan, H.-Y. Quercetin as a Potential Treatment for COVID-19-Induced Acute Kidney Injury: Based on Network Pharmacology and Molecular Docking Study. *PLoS One* **2021**, *16*, https://doi.org/10.1371/journal.pone.0245209.
41. Farhat, N.; Khan, A.U. Repurposing Drug Molecule against SARS-Cov-2 (COVID-19) through Molecular Docking and Dynamics: A Quick Approach to Pick FDA-Approved Drugs. *J Mol Model* **2021**, *27*, https://doi.org/10.1007/s00894-021-04923-w.
42. Chiou, W.-C.; Hsu, M.-S.; Chen, Y.-T.; Yang, J.-M.; Tsay, Y.-G.; Huang, H.-C.; Huang, C. Repurposing Existing Drugs: Identification of SARS-CoV-2 3C-like Protease Inhibitors. *J Enzyme Inhib Med Chem* **2021**, *36*, 147–153, https://doi.org/10.1080/14756366.2020.1850710.
43. Sonkar, C.; Doharey, P.K.; Rathore, A.S.; Singh, V.; Kashyap, D.; Sahoo, A.K.; Mittal, N.; Sharma, B.; Jha, H.C. Repurposing of Gastric Cancer Drugs against COVID-19. *Comput Biol Med* **2021**, *137*, https://doi.org/10.1016/j.compbiomed.2021.104826.
44. Sayed, A.M.; Khalaf, A.M.; Abdelrahim, M.E.A.; Elgendy, M.O. Repurposing of Some Anti-Infective Drugs for COVID-19 Treatment: A Surveillance Study Supported by an in Silico Investigation. *Int J Clin Pract* **2021**, *75*, https://doi.org/10.1111/ijcp.13877.
45. Al-Shar'i, N.A. Tackling COVID-19: Identification of Potential Main Protease Inhibitors via Structural Analysis, Virtual Screening, Molecular Docking and MM-PBSA Calculations. *J Biomol Struct Dyn* **2021**, *39*, 6689–6704, https://doi.org/10.1080/07391102.2020.1800514.
46. Shree, P.; Mishra, P.; Selvaraj, C.; Singh, S.K.; Chaube, R.; Garg, N.; Tripathi, Y.B. Targeting COVID-19 (SARS-CoV-2) Main Protease through Active Phytochemicals of Ayurvedic Medicinal Plants - Withania Somnifera (Ashwagandha), Tinospora Cordifolia (Giloy) and Ocimum Sanctum (Tulsi) - a Molecular Docking Study. *J Biomol Struct Dyn* **2022**, *40*, 190–203, https://doi.org/10.1080/07391102.2020.1810778.
47. Murugesan, S.; Kottekad, S.; Crasta, I.; Sreevathsan, S.; Usharani, D.; Perumal, M.K.; Mudliar, S.N. Targeting COVID-19 (SARS-CoV-2) Main Protease through Active Phytocompounds of Ayurvedic Medicinal Plants - Emblica Officinalis (Amla), Phyllanthus Niruri Linn. (Bhumi Amla) and Tinospora Cordifolia (Giloy) - A Molecular Docking and Simulation Study. *Comput Biol Med* **2021**, *136*, https://doi.org/10.1016/j.compbiomed.2021.104683.

48. Cai, Y.; Zeng, M.; Chen, Y.-Z. The Pharmacological Mechanism of Huashi Baidu Formula for the Treatment of COVID-19 by Combined Network Pharmacology and Molecular Docking. *Ann Palliat Med* **2021**, *10*, 3864–3895, https://doi.org/10.21037/apm-20-1759.
49. Gurung, A.B.; Ali, M.A.; Lee, J.; Farah, M.A.; Al-Anazi, K.M. Identification of Potential SARS-CoV-2 Entry Inhibitors by Targeting the Interface Region between the Spike RBD and Human ACE2. *J Infec Public Health* **2021**, *14*, 227–237, https://doi.org/10.1016/j.jiph.2020.12.014.
50. Abdalla, M.; Mohapatra, R.K.; Sarangi, A.K.; Mohapatra, P.K.; Eltayb, W.A.; Alam, M.; El-Arabey, A.A.; Azam, M.; Al-Resayes, S.I.; Seidel, V.; Dhama, K. In Silico Studies on Phytochemicals to Combat the Emerging COVID-19 Infection. *J Saudi Chem Soc* **2021**, *25*, https://doi.org/10.1016/j.jscs.2021.101367.
51. Dallakyan, S.; Olson, A.J. Small-Molecule Library Screening by Docking with PyRx. *Methods Mol Biol* **2015**, *1263*, 243–250, https://doi.org/10.1007/978-1-4939-2269-7_19.
52. Adeniji, S.E.; Arthur, D.E.; Oluwaseye, A. Computational Modeling of 4-Phenoxynicotinamide and 4-Phenoxypyrimidine-5-Carboxamide Derivatives as Potent Anti-Diabetic Agent against TGR5 Receptor. *J King Saud Univ Sci* **2020**, *32*, 102–115, https://doi.org/10.1016/j.jksus.2018.03.007.
53. Shin, D.; Mukherjee, R.; Grewe, D.; Bojkova, D.; Baek, K.; Bhattacharya, A.; Schulz, L.; Widera, M.; Mehdipour, A.R.; Tascher, G.; Geurink, P.P.; Wilhelm, A.; van der Heden van Noort, G.J.; Ovaa, H.; Müller, S.; Knobeloch, K.-P.; Rajalingam, K.; Schulman, B.A.; Cinatl, J.; Hummer, G.; Ciesek, S.; Dikic, I. Papain-like Protease Regulates SARS-CoV-2 Viral Spread and Innate Immunity. *Nature* **2020**, *587*, 657–662, https://doi.org/10.1038/s41586-020-2601-5.